IEEE Access
Multidisciplinary | Rapid Review | Open Access Journal

Received February 13, 2019, accepted March 19, 2019, date of publication April 22, 2019, date of current version May 13, 2019.

Digital Object Identifier 10.1109/ACCESS.2019.2909789

Quantitative Analysis for Networked Output Feedback MPC of Clock Synchronization in Unreliable WSN

TING WANG[1], JIE SHANG[2], AND XIAOMING TANG[2]

[1]Key Laboratory of Industrial Internet of Things & Networked Control, Chongqing University of Posts and Telecommunications (CQUPT), Chongqing 400065, China

[2]School of Automation, Chongqing University of Posts and Telecommunications, Chongqing 400000, China

Corresponding author: Ting Wang (wangting@cqupt.edu.cn)

This work was supported in part by the National Natural Science Foundation of China under Grant 61403055, Grant 51705059, and Grant 51605065, in part by the Chongqing Science and Technology Commission under Grant 2017jcyjAX0453, Grant cstc2018jcyjAX0691, and Grant cstc2018jcyjAX0139, in part by the Scientific and Technological Research Program of Chongqing Municipal Education Commission under Grant KJQN201800645, and in part by the Chongqing Education Administration Program Foundation of China under Grant KJ1600402.

ABSTRACT In the industrial cyber-physical environment, the performance of clock synchronization with loss of data packets should be analyzed quantitatively. The localized state estimator and controller are designed to realize the speed of convergence for exponential stability of the clock synchronization for the output feedback tubes-model predictive control (Tubes-MPC) of the state-space model. The upper and lower bounds for the variance of synchronization error under the statistical significance were quantitatively analyzed in incomplete measurement. The set of interference error in complete measurement was added into the set of additional estimated errors introduced by packet loss. Clock synchronization of the output feedback Tubes-MPC which has been constructed still has the performance of robust exponential convergence under networked packet loss, and it can be extended to an absolute state-space model with network-level in a unified approach.

INDEX TERMS Model predictive control, clock synchronization, state-space model, packet loss, synchronization accuracy, synchronization error.

I. INTRODUCTION

WHEN clock synchronization is completed in unreliable WSN [1], [2], [4], a lot of data packets with time message cannot successfully arrive in the specified observation period in the process of two-ways message observation, which is called incomplete measurement. The problem is that the random measurement variance introduced by the incomplete measurement will generate additional estimated error [4]–[6], resulting in clock synchronization error and convergence performance of network-level clock cannot be evaluated quantitatively.

Early studies of the clock synchronization used clock synchronization protocols in the Wireless Sensor Networks to estimate clock parameters and adjust synchronization [7]–[9]. The problem of clock synchronization in WSN is analyzed by using the view of statistical signal processing in [10], [12], [13]. The consensus algorithm compensates the collected states of neighboring nodes to their own states directly by adopting the maximum or minimum selection strategy which is uniform [3], [4], [11]. However, this method is easily affected by the size of network and the states of nodes, and the convergence speed is slow, especially when a large number of packet loss occur.

The engineering background of the paper is reflected in whether the convergent performance of the clock synchronization can be realized in controlled pattern. It can analyze the convergence speed and convergence error quantitatively, which is usually of important practical significance for deterministic industrial applications (Industrial Applications for hard real-time), IoT (Internet of Things), and 5G. For example, the on-line monitoring and acquisition of synchronous data for large-scale rotary intelligent equipment [18].

The associate editor coordinating the review of this manuscript and approving it for publication was Md. Arafatur Rahman.

This work is licensed under a Creative Commons Attribution 3.0 License. For more information, see http://creativecommons.org/licenses/by/3.0/

Literatures [5], [14] have proposed a state-space model of the relative clock of the clock synchronization in the previous studies, and established the framework of clock synchronization from the theory of Networked Control System. Making a balance among synchronization error and convergence speed in the application of clock synchronization in the control strategy of MPC (Model Predictive Control) based on [5], [14], we hope that we cannot only stand on the level of pure theoretical discussion to a certain degree (such as the particularity of the clock synchronization described in [14]), but also consider the difference of practical aspects between MPC and the traditional model predictive control used in industrial application. Algorithm of the clock synchronization in the Cyber-Physical environment needs better convergent stable error, accuracy which is quantized and adaptive to the size of the network, controllable convergence speed, and better robustness for packet loss.

The superiority of predictive control not only deals with industrial constraint problem, but also brings together the advantages of distributed model [23]. Inspired by the previous work, [22], [24] have addressed the DMPC for a set of linear local systems with decoupled dynamics and a coupled global cost function.

In industrial networking (including wireless smart devices embedded in wireless RF chips), the present paper hope to further improve the performance of clock synchronization enhancing DMPC when considering papers [27] on Robust and stochastic MPC. The on-line synthesis approaches of MPC have been investigated for NCS (Networked Control Systems) where the packet loss and data quantization are coexisting (see [25]) and network-induced delays (see [26]), and is the one which guarantees the closed-loop stability, i.e. the closed-loop system is stable whenever the optimization problem is feasible.

In the Cyber-Physical environment of the industrial Internet of Things [18], we have made further improvement for the industrial requirements of the large-scaled applications and the performance of online Tubes-MPC algorithm [18], [27]. Literatures [16], [17] have introduced the nominal system and adopted constraints of terminal region to realize steady-state convergence with constraints Tubes model predictive control. This control scheme has a simplified conditions of the Gaussian noise suitably. It has comprehensively studied the robustness and importance of random model predictive control in [27], and then it has pointed out that the researches of the model predictive control need to fully consider the industrial demands. The main focus is on robust and random model predictive control because MPC with these control forms often needs to solve complex problems of optimized control online. On the basis of solid theory, it is necessary to pay more attention to studies of the applicability of MPC in the specific industrial fields. Considering the constraints of terminal region, the present paper attempts to combine the KF-based MPC with the important Tubes-MPC to obtain some valuable researches.

Reference [15] has got on a rigorous and basic research on problems of control and estimation in the unreliable networks. B. Sinopoli and others have proved that there is a boundary for receiving rate of data packets by adopting the strategy of fully packet loss, so that the error covariance of the Kalman filter is convergent, and the upper and lower bounds of this important boundary value are given [6], [19]. In the previous study [5], the relationship between rate of packet loss and covariance matrix based on statistically significant has been drawn, and a method for calculating the minimum rate of packet loss under the requirement of meeting the synchronization accuracy has been designed from the perspective of energy consumption, which has practical value in the industrial applications.

The main contributions of the present paper are as follows:

1) The present paper established a Tubes-MPC method of clock synchronization for output feedback predictive control based on the view of networked control and the previous researches [5], [14];

2) The upper and lower bounds of variance under the statistical significance for the error variance of clock synchronization with packet loss is analyzed quantitatively, and it is mapped to the constraint set of the additional estimated error introduced by packet loss;

3) Based on the quantized relationship between the bounds of the variance for packet loss and arrival rate, the set of interference error in incomplete measurement is quantified, and the predictive optimal model is robust for performance of exponentially stable convergence of Tubes-MPC clock synchronization under networked packet loss.

II. STATE-SPACE MODEL OF CLOCK SYNCHRONIZATION

A. CLOCK MODEL

Nodes of each sensor in WSN have their own clocks, and the readings for clocks are represented by an integral model

$$c_i(t) = \int_0^t \beta_i(\tau)d\tau + \theta_i^0 \tag{1}$$

where $\beta_i(\tau)$ is the time varying skew of node i, and θ_i^0 is the initial clock offset of node i. The clock model is built into integral model because the clock crystal is not perfect in reality and can be affected by the environmental factors, so that the frequency for crystal oscillator of each node will change. Considering that the change of frequency for crystal oscillator has very little effect on clock synchronization in WSN in a short period of time, the clock reading $c_i(t)$ of sensor node i is represented by a linear model [14]:

$$c_i(t) = \beta_i(t) + \theta_i \tag{2}$$

where β_i is the clock skew of node i, θ_i is the clock offset of node i, when $\beta_i = 1$, $\theta_i = 0$, $c_i(t) = t$, the clock of node i is called the standard clock at this time. Since the standard time t cannot be obtained, the relative clock of node j which

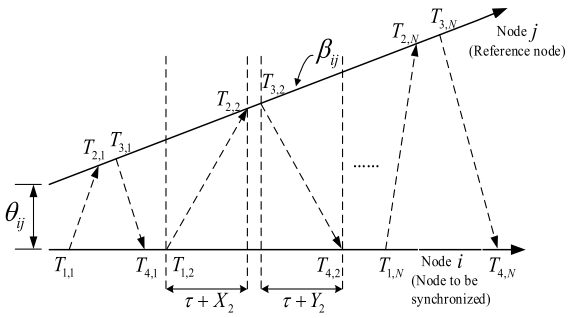

FIGURE 1. Exchange model of clock message between neighbor nodes at reference time.

is relative to node i is established as follows:

$$c_j(t) = \beta_j[\frac{c_i(t)-\theta_i}{\beta_i}] + \theta_j = \frac{\beta_j}{\beta_i}c_i(t) + [\theta_j - \frac{\beta_j}{\beta_i}\theta_i] = \beta_{ij}c_i(t) + \theta_{ij} \quad (3)$$

where β_{ij} is the relative clock skew and θ_{ij} is the relative clock offset of node j which is relative to node i.

B. ESTABLISHMENT OF OBSERVATION MODEL BASED ON TWO-WAYS MESSAGE EXCHANGE MECHANISM

In this paper, we use two-ways message exchange mechanism to exchange the clock message of adjacent two-nodes. As shown in Fig.1, it is assumed that the exchange of message of the clock synchronization between node i and node j takes place N rounds. During k-th round of message exchange, the set of time stamp obtained by node i is $\{T_{1,k}, T_{2,k}, T_{3,k}, T_{4,k}\}_{k=1}^{N}$, the above exchange process of timestamp message can be modeled as:

$$\begin{cases} T_{2,k} = \beta_{ij}(T_{1,k} + \tau + X_k) + \theta_{ij} \\ T_{3,k} = \beta_{ij}(T_{4,k} - \tau - Y_k) + \theta_{ij} \end{cases} \quad (4)$$

Among them, the random delays of clock message in the process of message exchange between node i and node j are X_k and Y_k; τ is the fixed delay in the exchange process.

Here, we need to make following assumptions:

1) Considering that X_k and Y_k are random variables. They are independent and identically distributed. If we assume that the random delay is an accumulation of numerous independent random processes, then X_k and Y_k will meet the Gaussian distribution according to the Central Limit Theorem. Reference [8] has confirmed that the confidence for constructing the random delay as a Gaussian distribution is 99.8%. Therefore, we assume that random delays X_k and Y_k obey the Gaussian distribution with zero mean and variance ${\sigma_v}^2$;

2) Suppose that fixed delay τ in equation (4) is symmetric, mainly based on following three points:

① We only consider the exchange of message between neighbors with no situation of multi-hop transmission in the present paper;

② The size and transmission rate of packets of time message exchanging between nodes are the same, so both nodes have the same time of transmission and arrival;

③ Assuming that relative position of two nodes has not changed during process of message exchange, so time of transmission between two nodes are the same [14];

3) We can estimate β_{ij} by statistical signal processing in the case where the fixed delay is known or unknown, and the method of system identification can be used due to slow time-varying characteristic of β_{ij} [5]. We assume that β_{ij} is constant and known in the period of current synchronization, but it can be different in different cycles, that is, in the k-th round of synchronization cycle, if we make $\beta_{ij} = {\beta_{ij}}^k$, $k = 1, 2, 3\ldots$, we can get ${\beta_{ij}}^{k+1} \neq {\beta_{ij}}^k$.

For above reasons, we choose $x = [\,\tau\ \theta_{ij}\,]^T$ as the system state, and the observation equation of node i which is relative to node j can be obtained based on equation (4):

$$y(k) = Cx(k) + v_k \quad (5)$$

where $y(k) = \left[T_{2,k}/\beta_{ij} - T_{1,k};\ T_{4,k} - T_{3,k}/\beta_{ij}\right]$; and $v_k = [X_k; Y_k]$ is the Gaussian distribution with zero mean, $Ev_kv_k^T = R \in \Re^{2\times2}$, $C = \left[1^1/\beta_{ij};\ 1 - 1/\beta_{ij}\right]_{2\times2}$.

Defining that γ_k describes packet loss for the k-th round of message exchange. $\gamma_k = 1$ when data is successfully exchanged between nodes, otherwise $\gamma_k = 0$. γ_k is a random event and is consistent with random process of the Bernoulli distribution if all roundsąŕ processes of message exchange are considered. At this time, there is $p(\gamma_k = 1) = \lambda$ for the Bernoulli variable γ_k in statistical sense [5], where λ represents the probability of packet arrival. The observation model (5) is modified as follows:

$$y(k) = Cx(k) + {v_k}' \quad (6)$$

where noise ${v_k}'$ becomes a variable about γ_k, ${v_k}' \sim N(0, \gamma_k R + (1-\gamma_k)\bar{\sigma}^2 I$, noise variance $\bar{\sigma}$ tends to infinity when the observed message is dropped.

The observation equation for state $x = \theta_{ij}$ in scalar form can be obtained by (4)

$$y(k) = Cx(k) + v_k \quad (7)$$

where $y(k) = \frac{T_{2k}+T_{3k}}{\beta_{ij}} - T_{1,k} - T_{4,k}$, $C = \frac{2}{\beta_{ij}}$, $v_k = X_k - Y_k$, $v_k \sim N(0, 2\sigma_v^2)$ and $Ev_kv_k^T = R \in \Re$.

Similarly, considering (6) in incomplete measurement, (7) is modified as follows:

$$y(k) = Cx(k) + {v_k}' \quad (8)$$

Same symbolic representation and consistent mathematical model is used for vector observation model (6) and scalar observation model (8), only the dimension is inconsistent, but it does not affect the discussion in the present paper.

C. ESTABLISHMENT OF STATE-SPACE MODEL

In section II-B, we has obtained the state observation model of clock synchronization. In this section we will establish another core part of the state-space model, a model for state updating.

As mentioned in observation model (6), state vector consists of the fixed delay τ and relative clock offset θ_{ij} and the

two parameters of the vector are unknown. Assuming that the current state is linear to state at the previous moment, because of its slow change, the unknown state is built as Gauss-Markov dynamic model [14]:

$$x(k) = Ax(k-1) + w_k \tag{9}$$

where A is a 2×2 unit matrix; each of terms in w_k obeys the Gaussian distribution with zero mean and variance σ_w, $Ew_k w_k^T = Q \in \Re^{2\times 2}$.

In this paper, we attempt to establish a theoretical basis based on the estimation and control for problems of clock synchronization in unreliable WSN. This method is independent of networked nodes distribution and method of communication, it is a systematic method which can adapt to networked changes. We can produce an optimal control input $u(k)$ to modify logic clock of node i quoting theory of modern control. This change of state can be abstracted as:

$$x(k) = Ax(k-1) + Bu(k-1) + w_k \tag{10}$$

where $A = 1$, B is matrix of control weight, $Ew_k w_k^T = Q \in \Re^{2\times 2}$.

It is feasible to ignore fixed delay τ since the most closely related amount of clock synchronization is the relative clock offset from section II-B. When the state is selected as $x = \theta_{ij}$, the state change in scalar form is:

$$x(k) = Ax(k-1) + Bu(k-1) + w_k \tag{11}$$

where $A = 1$; B is the first-order matrix of control weight.

At this point, we obtain the equations of state updating and observation of clock synchronization, it can be described with following unified description as follows:

$$\begin{cases} x(k) = Ax(k-1) + Bu(k-1) + w_k \\ y(k) = Cx(k) + v_k{}' \end{cases} \tag{12}$$

(12) defines two kinds of state-space model in different states respectively. We can call the vector model of state $x = [\,\tau\ \theta_{ij}\,]^T$ as model 1, and the scalar model at state $x = \theta_{ij}$ as model 2. Due to the uncertainty of WSN, regardless of which model is used, the key issue is the choice of methods for state estimation and control strategies in incomplete measurement.

III. ANALYSIS OF SYNCHRONIZATION ACCURACY FOR KALMAN FILTER IN INCOMPLETE MEASUREMENT

If too much observations are dropped, the process of the Kalman filter will be unstable. If the estimation of clock parameter is inaccurate, the synchronization of logical clock will not be achieved. Considering the loss of observed value, we need to re-establish the estimated model of Kalman filter, analyze the iterative process of error covariance, and discuss the arrival rate λ and convergence of expectation for covariance matrix.

According to state-space model (12) we can express Kalman filter equation as:

$$\hat{x}(k+1|k) = A\hat{x}(k|k) + Bu(k) \tag{13}$$

$$P(k+1|k) = AP(k|k)A^T + Q \tag{14}$$

$$P(k+1|k+1) = P(k+1|k) - \gamma_{k+1}K_{k+1}CP(k+1|k) \tag{15}$$

$$\hat{x}(k+1|k+1) = \hat{x}(k+1|k) + \gamma_{k+1}K_{k+1}[y(k+1) - C\hat{x}(k+1|k)] \tag{16}$$

$$K(k+1) = P(k+1|k)C^T[CP(k+1|k)C^T + R]^{-1} \tag{17}$$

From equations (13) to (17), correlation equations for Kalman filter are not affected by the model we used. According to (14), (15) and (17), we can get a recurrence equation of prior error matrix

$$P(k+1|k) = AP(k|k-1)A^T + Q - \gamma_k AP(k|k-1)C^T\Big[CP(k|k-1)C^T + R\Big]^{-1}CP(k|k-1)A^T \tag{18}$$

We can make $P_k = P(k|k-1)$, then:

$$P_{k+1} = AP_kA^T + Q - \gamma_k AP_kC^T\Big[CP_kC^T + R\Big]^{-1}CP_kA^T \tag{19}$$

P_k becomes a random variable about γ_k which is an uncertain quantity, so we mainly discuss the convergence properties of $\lim_{k\to\infty} E[P_k]$ in statistical significance.

$$E[P_{k+1}] = AE[P_k]A^T + Q - \lambda E[AP_kC^T\Big(CP_kC^T + R\Big)^{-1}CP_kA^T] \tag{20}$$

Defining a modified algebraic Riccati equation as:

$$g_\lambda(X) = AXA^T + Q - \lambda AXC^T\Big(CXC^T + R\Big)^{-1}CXA^T \tag{21}$$

To simplify the proof of following theorems, the auxiliary function can be given as:

$$\Phi(K, X) = (1-\lambda)(AXA^T + Q) + \lambda\Big(FXF^T + V\Big) \tag{22}$$

where $F = A + KC$, $V = Q + KRK^T$, and there is $g_\lambda(X) = \Phi(K_X, X)$ when $K_X = -AXC^T\big[CXC^T + R\big]^{-1}$.

Reference [6] has discussed relative properties of modified algebraic Riccati (21), such as Lemma 1 which proves convergence of (21). In this section, we will mainly prove that matrix $E[P_k]$ of error covariance in statistical sense (i.e., the expectation about P_k) is bounded by using this conclusion and calculate its boundary.

Lemma 1: *The Convergence Properties of Riccati Equation*

Suppose there are matrix $\widehat{K}$ and positive semi-definite matrix $\widehat{P}$, satisfying $\widehat{K} > 0$ and $\widehat{P} > \Phi(\widehat{K}, \widehat{P})$, then there is $\lim_{k\to\infty} P_k = \lim_{k\to\infty} g_\lambda^k(P_0) = \bar{P}$ for any initial value $P_0 > 0$, the convergence value $\bar{P}$ is independent of initial value and $\bar{P}$ is the only positive definite solution of Riccati (21).

Quantitative Analysis of Boundary for Expectation of Error Covariance

If $\left(A, Q^{1/2}\right)$ is controllable, (A, C) can be measured, $\lambda > \lambda_c$, then there are $0 < S_k \leq E[P_k] \leq V_k$, $\lim_{k\to\infty} S_k = \bar{S}$ and $\lim_{k\to\infty} V_k = \bar{V}$ when $\forall E[P_0] \geq 0$, where $\bar{S}$ is the solution of $\bar{S} = (1-\lambda)A\bar{S}A^T + Q$, $\bar{V}$ is the solution of $\bar{V} = g_\lambda(\bar{V})$, and λ_c is the critical arrival rate, $\lambda_c \in [0, 1]$.

Proof: If $V_k = P_k$, according to Lemma 1 we will see that $\lim_{k\to\infty} V_k = \bar{V}$, $\bar{V} = g_\lambda(\bar{V})$. Considering sequence $V_{k+1} = g_\lambda(V_k)$, $V_0 = E[P_0] \geq 0$, if $E[P_k] \leq V_k$, then $E[P_{k+1}] = E[g_\lambda(P_k)] \overset{a}{\leq} g_\lambda(E[P_k]) \leq V_{k+1}$, where the inequality a is established mainly by the Jensen inequality. By induction, we can get that there are $V_k \geq E[P_k]$ for $\forall k$.

If the observation matrix C is reversible, the exact value of λ_c can be calculated from literature [5]. Matrix C in model 1 and model 2 is full rank in this paper, if $\lambda > \lambda_c$, then there exists $\widehat{X}$ to meet $\widehat{X} \geq g_\lambda(\widehat{X})$. For $\forall k$, there are $S_k \leq E[P_k] \leq V_k$.

Set the initial value as $E[P_0] \geq 0$, then we can get $0 = S_0 \leq E[P_0]$, there is $S_{k+1} \leq (1-\lambda)AE[P_k]A^T + Q \leq E[g_\lambda(P_k)] = E[P_{k+1}]$.

For $\forall k$, there are $S_k \leq E[P_k]$. Since S_k is a monotonically increasing sequence, S_k has a boundary with $S_k \leq V_k \leq M$, i.e. $\lim_{k\to\infty} S_k = \bar{S}$.

Due to the randomness of γ_k, we will discuss the convergence properties of expectation for P_k, and the boundary of $E[P_k]$ reflects a measure of deviation between state estimation $\hat{x}$ and state x of disturbance system, which establishes a relationship between arrival rate of packets and system state. In this paper, we will use this kind of contact to design controller and enhance the robustness of controller for packet loss and reduce synchronization error.

IV. DESIGN OF TUBES MODEL PREDICTIVE CONTROLLER

A. ESTIMATED AND CONTROL ERRORS

When packet loss occurs, the upper bound of the covariance in statistical sense obtained by section III reflects the maximum measure of the average of deviation between the disturbance system state and estimated system state:

$$\varphi(-\sqrt{V_k}) \leq x_k(i) - \hat{x}_k(i) \leq \varphi(\sqrt{V_k}), x_k(i) \in X, \quad \forall i \in N_{N_c-1} \tag{23}$$

where $\varphi(\cdot)$ is a column vector composed of data in the upper left corner and the lower right corner of corresponding input matrix obtained by function mapping.

In fact, (23) is not always established. Conditions may be too conservative or unsatisfactory for system in each operation. Directly discuss the conditions for establishment of such inequality, we cannot draw an accurate upper and lower bounds of inequality in the case of packet loss. Although condition (23) is not always satisfied in incomplete measurement, the state is still in the state set X, and it will not cause the situation that $P_{N_c}(\hat{x}(k))$ will not have any solution. In complete measurement, such upper and lower bounds can be obtained by minimum invariant set $\tilde{S}$ [21], then in incomplete measurement:

$$\tilde{x}_k(i) \in \tilde{S}^+ \supseteq \tilde{S} \tag{24}$$

We have obtained the relationship between different rates of packet loss and the upper bound of the covariance from Section III. For set $\tilde{S}$, if it is expanded to $\tilde{S}^+$ with corresponding rate of packet loss $1-\lambda$, there exists:

$$\tilde{S}^+ - \tilde{S} = \Delta \tag{25}$$

$\Delta = \left[\varphi\left(-\sqrt{\bar{V}}\right), \varphi\left(\sqrt{\bar{V}}\right)\right]_{1-\lambda} - \left[\varphi\left(-\sqrt{\bar{V}}\right), \varphi\left(\sqrt{\bar{V}}\right)\right]_{\lambda=1}$, $\left[\varphi\left(-\sqrt{\bar{V}}\right), \varphi\left(\sqrt{\bar{V}}\right)\right]_{1-\lambda}$ is the border of the corresponding rate of packet loss $1-\lambda$.

Therefore, it is important to firstly discuss the relative invariant set and design of controller in complete measurement, which will offer the design basis for design of controller in the case of packet loss. The state-space model of the disturbance system in complete measurement is:

$$\begin{cases} x(k) = Ax(k-1) + Bu(k-1) + w_k \\ y(k) = Cx(k) + v_k \end{cases} \tag{26}$$

The control is constrained to $u_s(k) \in U$, $u_s(k) \triangleq \{u_k(0), u_k(1), \ldots, u_k(i), \ldots, u_k(N_c-1)\}$ is a set of control sequence predicted at the current time, $u(k) = u_k(0)$. (25) is constrained to following state and control set:

$$(x, u) \in X \times U \tag{27}$$

Process the noise w_k and measurement noise v_k are both subject to the normal distribution. The process noise w_k and measurement noise v_k can be constrained as follows with probabilities p_w and p_v based on probability theory:

$$P\{w_k \in W\} = p_w, P\{v_k \in V\} = p_v \tag{28}$$

where $P\{\cdot\}$ represents the function of probability distribution. In actual process, the process noise w_k and measurement noise v_k are constrained as follows with 99.97% probability according to 3σ rule:

$$P\{w_k \in W_{3\sigma}\} = 99.97\%, P\{v_k \in V_{3\sigma}\} = 99.97\% \tag{29}$$

where $W_{3\sigma} = [-3\sigma_w', 3\sigma_w']$, $V_{3\sigma} = [-3\sigma_v', 3\sigma_v']$, σ_w' and σ_v' are the variance of process noise and measured noise respectively for corresponding model.

In order to ensure that the computational complexity can be reduced under the premise of establishing relevant stability constraints, we use the non-delayed Luenberger observer, which is consistent with the unanimous expression of the Kalman filter observer in this section. For the estimated system:

$$\begin{cases} \hat{x}(k) = A\hat{x}(k-1) + Bu(k-1) + L[y(k-1) - \hat{y}(k-1)] \\ \hat{y}(k) = C\hat{x}(k) \end{cases} \tag{30}$$

where $\hat{x}(k)$ is the observation state at the current k-moment and L is the gain of observer.

The estimated error $\tilde{x} = x - \hat{x}$ of disturbance system and estimated system satisfies:

$$\tilde{x}(k) = A_L\tilde{x}(k-1) + (w_k - Lv_{k-1}), A = A - LC \quad (31)$$

where A_L satisfies $\rho(A_L) < 1$ and guarantees that equation (30) is stable.

In order to make the state of disturbance system and associated control always satisfy the constraint (27), a third dynamic nominal system is introduced. The nominal system is about to remove the relevant noise in disturbance system:

$$\bar{x}(k) = A\bar{x}(k-1) + B\bar{u}(k-1) \quad (32)$$

We can make $\bar{\phi}(i; \bar{x}(k), \bar{u}(k))$ be the state of system (32) at the i-th prediction step, the initial state is $\bar{x}(k)$. A set of control sequence $\bar{u}_s(k) \triangleq \{\bar{u}_k(0), \ldots, \bar{u}_k(N_c-1)\}$, $\bar{u}(k) = \bar{u}_k(0)$ is produced, which is corresponding to state sequence $\bar{x}_s(k) \triangleq \{\bar{x}_k(0), \ldots, \bar{x}_k(N_c)\}$. This sequence is the center point of the tube control that will be used in this paper.

In order to offset the disturbance, we add feedback part to the model predictive controller, and obtain the controller of disturbance system as follows:

$$u(k) = \bar{u}(k) + \bar{K}e(k) \quad (33)$$

where $e(k) \triangleq \hat{x}(k) - \bar{x}(k)$ is the corresponding control of nominal system.

The difference equation between estimated system and nominal system control error $e(k)$ is:

$$e(k) = A_{\bar{K}}e(k-1) + [LC\tilde{x}(k-1) + Lv_{k-1}] \quad (34)$$

where $A_{\bar{K}} \triangleq A + B\bar{K}$, which satisfies $\rho(A + B\bar{K}) < 1$.

The error between observed state and nominal state is $e(k)$, and the error between real state and observed state is $\tilde{x}(k)$:

$$x(k) = \bar{x}(k) + e(k) + \tilde{x}(k) \quad (35)$$

Defining that when a set $\bar{\Omega} \subset \mathcal{R}^n$ satisfies $\bar{x} \in \bar{\Omega}$ and $\bar{\Omega} \subseteq \bar{X}$, then the set $\bar{\Omega}$ is the positive definite invariant set [21] of state $\bar{x}$ of system (32).

Lemma 2 (The Set of State Estimated Error [17]): There is a positive definite invariant set $\tilde{S}$ for estimated error (31). If the initial state of disturbance system and estimated system satisfies $\tilde{x}(0) = x(0) - \hat{x}(0) \in \tilde{S}$, then there are $\tilde{x}(0) = x(0) - \hat{x}(0) \in \tilde{S}$, that is $x(k) \in \hat{x}(k) \oplus \tilde{S}$.

For the solution of set $\tilde{S}$ for estimated error, it cannot obtain the exact calculation method in actual process, so it discusses the iterative method to obtain approximate solution $\tilde{S}$ in [23].

Lemma 3 (The Set of Control Error [17]): There is a positive definite set $\bar{S}$ for the control error (34). If the initial state of estimated system and the nominal system satisfies $e(0) = \hat{x}(0) - \bar{x}(0) \in \bar{S}$, then there are $e(k) \in \bar{S}$, i.e.$\hat{x}(k) \in \bar{x}(k) \oplus \bar{S}$, for $\forall w_k \in W$, $\forall v_k \in V$.

Lemma 4 (The Set of Interference Error [17]): Defining the set of interference errors $S = \tilde{S} \oplus \bar{S}$, if the initial error is $\tilde{x}(0) \in \tilde{S}$ with $e(0) \in \bar{S}$, then there are $x(k) \in \hat{x}(k) \oplus \tilde{S} \subseteq \bar{x}(k) \oplus S$.

Set $\tilde{S}$ quantifies the deviation between estimated system and state of disturbance system caused by system noise during each step of the control process. Set $\bar{S}$ establishes relationship of set constraint between estimated system and nominal system.

(See literature [17] for proof of lemmas 2,3,4.)

B. DESIGN OF CONTROLLER

In traditional model predictive control, the problem of control in disturbance system can be directly solved. The control cannot fully overcome noise disturbance because of existence of noise. Considering the abstract nominal system, there is no noise for $\bar{x}(0) = \hat{x}(0|0)$, and the requirements of control performance for disturbance system can be predicted in advance by acting the feedback control $u(k) = \bar{u}(k) + \bar{K}e(k)$ based on nominal system on disturbance system. In order to ensure that the control of nominal system $\bar{u}(k)$ is available for disturbance system, it is necessary to make some additional constraints on the state and control.

Let $\bar{x}_k(i) = \bar{x}(k+i)$, the objective function of control problem for nominal system $P_{N_c}[\bar{x}(k)]$ is:

$$V_{N_c}(\bar{x}_s(k), \bar{u}_s(k)) \triangleq \sum_{i=0}^{N_c-1} \ell(\bar{x}_k(i), \bar{u}_k(i)) + V_f(\bar{x}_k(N_c)) \quad (36)$$

The state $\bar{x}$ and control $\bar{u}$ of nominal system are constrained to the following reduction set:

$$(\bar{x}, \bar{u}) \in \bar{X} \times \bar{U}, \bar{X} \triangleq X - S, \bar{U} \triangleq U - \bar{K}\bar{S} \quad (37)$$

Defining terminal status $\bar{x}_k(N_c)$ of the system should meet the following conditions:

$$\bar{x}_k(N_c) \in X_f \quad (38)$$

where X_f satisfies the stability conditions.

According to equations (37) and (38), when state $\bar{x}(k)$ of nominal system is given, such a set of control sequence $\bar{u}_s(k)$ will be calculated:

$$\tilde{u}_{N_c}(\bar{x}(k)) = \{\bar{u}_s(k) | \bar{u}_k(i) \in \bar{U},\ \bar{x}_k(i) \in \bar{X},\ \forall i \in N_{N-1},\ \bar{\phi}(N_c; \bar{x}(k), \bar{u}(k)) \in X_f\} \quad (39)$$

The definition region $\bar{X}_{N_c}$ of function $V_{N_c}(\bar{x}_s(k), \bar{u}_s(k))$ can be defined as:

$$\bar{X}_{N_c} = \{\bar{x} | \tilde{u}_{N_c}(\bar{x}(k)) \neq \emptyset\}$$

At this point, we have obtained all conditions and expressions for solving the optimal control problem of nominal system. The optimal control solution $P_{N_c}[\hat{x}(k)]$ for estimated system is expressed as follows:

$$V_{N_c^*}(\hat{x}(k)) \triangleq \min_{\bar{x},\bar{u}} \{V_{N_c}(\bar{x}_s(k), \bar{u}_s(k)) | \bar{u}(k) \times \in \tilde{u}_{N_c}(\bar{x}(k)), \hat{x}(k) \in \bar{x}(k) \oplus \bar{S}\} \quad (40)$$

$$(\bar{x}^*(\hat{x}(k)), \bar{u}^*(\hat{x}(k))) = \arg\min_{\bar{x},\bar{u}} \{V_{N_c}(\bar{x}_s(k), \bar{u}_s(k)) \times \bar{u}(k) \in \tilde{u}_{N_c}(\bar{x}(k)), \hat{x}(k) \in \bar{x}(k) \oplus \bar{S}\} \quad (41)$$

Solving the optimal control problem $P_{N_c}[\hat{x}(k)]$, it will produce a set of optimal control sequence:

$$\bar{u}_s^*(\hat{x}(k)) \triangleq \{\bar{u}^*(\hat{x}(k),0),\cdots,\bar{u}^*(\hat{x}(k),N_c-1)\}$$

where $\bar{u}^*(k) \triangleq \bar{u}^*(\hat{x}(k),0)$ is the control of nominal system. It obtains a set of sequence of optimal state at the same time:

$$\bar{x}_s^*(\hat{x}(k)) \triangleq \{\bar{x}^*(\hat{x}(k),0),\cdots,\bar{x}^*(\hat{x}(k),N_c)\}$$

$\bar{x}^*(k) \triangleq \bar{x}^*(\hat{x}(k),0) = \bar{x}^*(\hat{x}(k))$ is the optimized nominal system state. From (25), we know that $\tilde{S}^+ = \tilde{S} \oplus \Delta$ in incomplete measurement is used to replace $\tilde{S}$ of the constraints in (37) and (38), and the set S of interference error is calculated into the set of additional estimated errors introduced by packet loss, then we can get the set S^+.

C. PROOF OF STABILITY WITHOUT PACKET LOSS

Firstly, according to definition of robust exponential stability, if the initial control error and the estimated error satisfy $e(0) \in \bar{S}$ and $\tilde{x}(0) \in \tilde{S}$ respectively, and the objective function $V_{N_c}(\cdot)$ satisfies properties in Lemma 7, then the control strategy $u^*(k) = \bar{u}^*(k) + \bar{K}(\hat{x}(k) - \bar{x}^*(k))$ is applied to disturbance system and estimated system, and the control strategy $\bar{u}^*(k)$ is applied to nominal system while solving the optimal control problem $P_{N_c}[\hat{x}(k)]$. The nominal system will exponentially converge to the target Z, and the estimated system and disturbance system will exponentially converge to sets $\bar{S} \oplus Z$ and $S \oplus Z$ respectively. (See appendix A for lemmas 5,6,7.)

Proof: according to definitions of $V_{N_c}(\cdot)$ and $V_{N_c}^*(\cdot)$, if $\bar{x}_i(k) = \bar{x}_i^*(\hat{x}_i(k))$, there are $V_{N_c}(\bar{x}_i^*(\hat{x}_i(k))) = V_{N_c}^*(\hat{x}_i(k))$. Then according to Lemma 7, $V_{N_c}^*(\hat{x}(k))$ satisfies:

$$\begin{aligned} &V_{N_c}^*(\hat{x}(k)) \\ &\quad = V_{N_c}^0(\bar{x}^*(\hat{x}(k))) \geq c_1|\bar{x}^*(\hat{x}(k)) - Z|^2, \quad \forall \hat{x}(k) \in X_{N_c} \\ &V_{N_c}^*(\hat{x}(k)) \\ &\quad = V_{N_c}^0(\bar{x}^*(\hat{x}(k))) \leq c_2|\bar{x}^*(\hat{x}(k)) - Z|^2, \quad \forall \hat{x}(k) \in X_f \oplus \bar{S} \end{aligned}$$

$$\begin{aligned} &V_{N_c}^*(\hat{x}(k+1)) - V_{N_c}^*(\hat{x}(k)) \\ &\quad \leq -c_1|\bar{x}^*(\hat{x}(k)) - Z|^2, \quad \forall \hat{x}(k) \in X_{N_c} \end{aligned}$$

According to the above relationship, we can know that:

$$V_{N_c}^*(\hat{x}(k+1)) \leq (c_2 - c_1)|\bar{x}^*(\hat{x}(k)) - Z|^2 \leq (c_2/c_1 - 1) V_{N_c}^*(\hat{x}(k))$$

Making $c = c_2/c_1 - 1$ and $|\bar{x}_i^*(\hat{x}_i(k)) - Z|^2 \leq 1/c_1 V_{N_c}^*(\hat{x}_i(k))$, then:

$$\begin{aligned} |\bar{x}^*(\hat{x}(k)) - Z|^2 &\leq 1/c_1 V_{N_c}^*(\hat{x}(k)) \leq 1_{c_1} c V_{N_c}^*(\hat{x}(k-1)) \\ &\leq \cdots \leq 1/c_1 c^k V_{N_c}^*(\hat{x}(0)) \leq c_2/c_1 c^k |\bar{x}^*(\hat{x}(0)) - Z|^2 \end{aligned} \tag{42}$$

So far, we have got $|\bar{x}^*(\hat{x}(k)) - Z| \leq \tilde{c}\delta^k |\bar{x}^*(\hat{x}(0)) - Z|$, where $\tilde{c} = \sqrt{c_2/c_1}$, $\delta = \sqrt{c}$, $c = c_2/c_1 - 1 \in (0,1)$. According to definition of exponential convergence, the nominal system exponentially converges to the balance point Z. Then, according to lemmas 2, 3 and 4, there are $\hat{x}(k) \in \bar{x}(k) \oplus \bar{S} = Z \oplus \bar{S}$ and $x(k) \in \bar{x}(k) \oplus \tilde{S} \oplus \bar{S} = Z \oplus S$ for estimated system and disturbance system respectively.

Kalman filter has a convergent performance which is close to CRLB (Cramer-Rao Lower Bound, CRLB) and a smaller estimated error than the Luenberger observer. For set $\tilde{S}'$ of state estimated error which uses the gain of Kalman filter, $\tilde{S}' \subseteq \tilde{S}$ is satisfied. Thus, the state $\hat{x}(k|k)$ obtained by Kalman filter also satisfies the set constraints calculated from the static gain , which ensures the feasibility of optimal control problem $P_{N_c}[\hat{x}(k|k)]$. The algorithm steps are shown in Table 1.

TABLE 1. Algorithm of Tubes model predictive control.

For any node i in the WSN

1. Initialize parameters: initialize the estimated value $\hat{x}(0|0)$ of clock parameter, covariance matrix $P_{N_{[i]}}(0|0)$ of error and initial control value $u(0|0)$. Select $\hat{x}(0) \in x(0) \oplus (-\tilde{S})$, set;
2. for $k = 1, 2, \ldots$ do
3. Run the Kalman filter to obtain estimation $\hat{x}(k|k)$ of optimal parameter;
4. Solve the problem$P_{N_c}(\hat{x}(k|k))$ of optimal control, then get the current nominal control $\bar{u}_i^*(k)$ and disturbance system control $u^*(k) = \bar{u}^*(k) + K(\hat{x}(k|k) - \bar{x}^*(k))$;
5. Control $u^*(k)$ is used to control the disturbance system and estimated system;
6. Calculate the next state $\bar{x}(k+1) = A\bar{x}(k) + B\bar{u}^*(k)$ of nominal system;
7. End for

D. PROOF OF STABILITY WITH PACKET LOSS

From lemmas 2,3 and 4, in the case of packet loss, there are positive sets $\tilde{S}^+$, $\bar{S}$ and $S^+ \triangleq \tilde{S}^+ \oplus \bar{S}$ satisfy $\tilde{x}(0) = x(0) - \hat{x}(0) \in \tilde{S}^+, \hat{x}(k) \in \bar{x}(k) \oplus \bar{S}$ and $x(k) \in \hat{x}(k) \oplus \tilde{S}^+ \subseteq \bar{x}(k) \oplus S^+$ respectively.

In the case of considering packet loss, if the initial control error and the estimated error satisfy $e(0) \in \bar{S}$ and $\tilde{x}(0) \in \tilde{S}^+$ respectively, due to the fact that the nominal system exponentially converges to the target Z is proved (as shown in IV-C), according to the inferences of lemmas 2, 3 and 4, there are $\hat{x}(k) \in \bar{x}(k) \oplus \bar{S} = Z \oplus \bar{S}$ and $x(k) \in \bar{x}(k) \oplus \tilde{S}^+ \oplus \bar{S} = Z \oplus S^+$ for estimated system and disturbance system respectively. So the estimated system and disturbance system will exponentially converge to sets $Z \oplus \bar{S}$ and $Z \oplus S^+$ respectively. (See appendix A for inferences of lemmas and their proof.)

V. SIMULATION AND PERFORMANCE EVALUATION

The nodesąŕ clock is directly compensated by estimated value according to protocol for classic clock synchronization in TPSN for protocol compensation mentioned in this section [7].

For model 2 with the scalar form, we consider clock synchronization with high precision. Set the initial value of the state at $x(0)= 0.012$ and the estimated initial value at $\hat{x}(0)= 0.02$. The control weight is $B= 1$, the initial covariance is $P(0) = E[(x(0) - \hat{x}(0))(x(0) - \hat{x}(0))^T]$. The covariance of the process noise w_k and measurement noise v_k are $Q = 10^{-5}$ and $R = 1.8 * 10^{-3}$ respectively. The target of clock synchronization is $Z = 0$. It represents the relative clock offset among nodes is zero, that is, the clock between nodes is synchronous. The observation matrix is $C = 1$. For algorithm of model predictive control, we choose $Q_\ell= 1$, $R_\ell= 0.5$. The prediction region $N_c= 1$, the state is constrained to $X \triangleq \{x \in R^1 | x \in [-0.1, 0.1]\}$, and the control is constrained to $U \triangleq \{u \in R | |u| \leq 0.012\}$. The gain of control $\bar{K}$ and the terminal penalty matrix are $\bar{K} = 1, P = 1$.

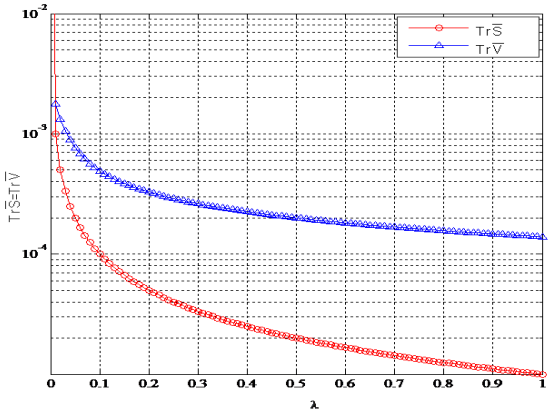

FIGURE 2. Upper and lower bounds of covariance asymptotic convergence under different packet arrival rates.

A. ANALYSIS OF SYNCHRONIZATION ACCURACY UNDER DIFFERENT ARRIVAL RATES

(1) Fig.2 is shown for this section. For model 2, the eigenvalue of A is 1. It can be seen that Kalman filter is still stable even if all observation values are dropped from [5], but the accuracy of clock synchronization is low due to the fully loss of observation values. Therefore, in this section, we analysis the boundary of the expectation of the error covariance by using Matlab.

Fig.2 shows the relationship between arrival rate λ of packets and $Tr\bar{V}$ and $Tr\bar{S}$. When $\lambda = 0.01$, $Tr\bar{V}$ and $Tr\bar{S}$ converge to 10^5. As the arrival rate λ of packets increases gradually, the trace of upper bound $\bar{V}$ and lower bound $\bar{S}$ are gradually reduced. The upper bound $Tr\bar{V}$ decreases by one order of magnitude when the arrival rate of packets λ gradually changes from 0.01 to 1, while the lower bound $Tr\bar{S}$ drops by nearly two orders of magnitude, indicating that the more clock information the node to be synchronized receives, the higher the accuracy of clock synchronization is. In this paper, we use the upper bound V_k as constraint condition of output feedback model to predict control. On the basis of obtaining the boundary, we further use Fig.9 platform for verification.

B. COMPARISON OF SYNCHRONIZATION ERROR AND CONVERGENCE SPEED UNDER DIFFERENT APPROACHES

(1) Fig.3 is shown for this section. The error of clock synchronization is generally measured by the error of clock parameter, which is a very significant and important indicator of clock synchronization performance. The error of clock synchronization for the k-th cycle of synchronization is defined as:

$$E(k) = \frac{1}{M}[\xi_i(k) - z_i]$$

where M is the number of experiments; ξ_i represents the i-th state quantity in state x, and z_i represents the i-th target quantity in target Z.

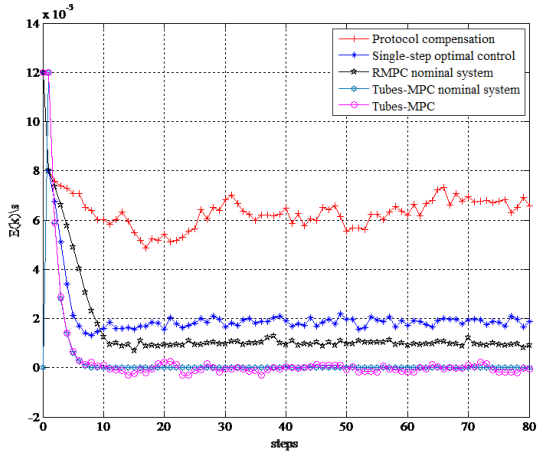

FIGURE 3. Comparison of $E(k)$ under different algorithms.

Fig.3 reflects the comparison of synchronization error among protocol compensation, single-step optimal control and the algorithm based on output feedback model predictive control when we use model 2 in complete measurement. The parameters of the single-step optimal control in experiments are set as $B = 1$, $D= 4$. It carries out 80 times two-ways message exchange in each round of clock synchronization, and a total of $M = 10$ times experiments are performed.

Comparing protocol methods of two-ways message exchange in [12], [13] (refer to method of protocol compensation for TPSN two-ways message exchange in [10]), it can be seen that synchronization error of the protocol compensation fluctuated around 6×10^{-3} from Fig.3, the algorithm of protocol compensation has larger error of synchronization than the output feedback model predictive control and single-step optimal control. The RMPC also converges in subsequent 5 steps and has a lower steady-state error of clock synchronization. It can be seen from Fig.3 that the Tubes-MPC reaches steady state at step 10 and then it continues

fluctuating near 0. Since the nominal system has no noise effect, the Tubes-MPC nominal system converges to 0 in step 9, and then keeps the value at 0, which is consistent with the result of quantitative analysis of exponential convergence.

Therefore, Tubes-MPC achieves faster convergence and has steady-state error of lower synchronization in this paper.

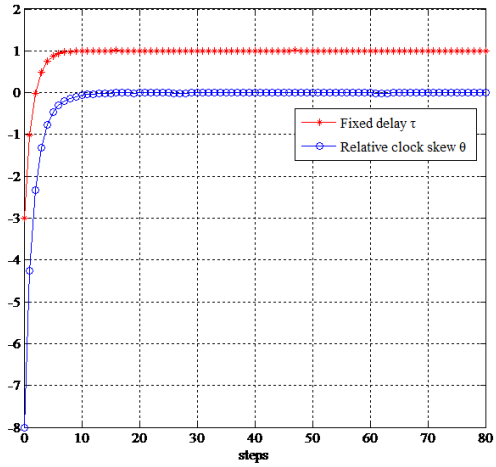

$$x(0) = [-3; -8], Z = [1; 0]$$

FIGURE 4. Effectiveness of Tubes-MPC exponential convergence for vector system.

(2) Fig.4 is shown for this section. In order to reflect the effectiveness of Tubes-MPC exponential convergence for vector system, Fig.4 uses Model 1 to run Tubes-MPC. The initial covariance is still calculated by using the method described above, $C = [11; 1-1]_{2\times 2}$, the weight of control $B{=}I_{2\times 2}$, the gain of control $\bar{K} = -[10; 01]_{2\times 2}$, for other parameters, they should multiply by $I_{2\times 2}$ to expand in accordance with the parameters in model 2.

In Fig.4, although the initial and estimated value of disturbance system state have large deviation, it exponentially converges to vicinity of the target value after step 9. Fig.4 shows that the state will not accurately reach the target value, it keeps fluctuating at a certain range. On the one hand, this phenomenon is due to the impact of noise, on the other hand, it mainly considers the dependence of Tubes-MPC for initial value of the state in Fig.4. According to the analysis of exponential convergence, it will be reasonable as long as the state converges to the set S. We only changed the initial state to [3; 2], then the same simulation result as Fig.4 can be obtained. Therefore, the clock state has no dependency on the initial value of the state under the control of Tubes-MPC.

(3) Fig.5 is shown for this section. In order to reflect that the state of system can be exponentially stable in set S more intuitively, when the initial point is $x(0) = [3; 2]$ as shown in Fig.5, the state of disturbance system is converged into S without showing the transition states before step 6. Set S quantifies the fluctuation range after the steady state of controlled disturbance system. we changed the initial point to $[-3; -8]$ and got the same simulation result as Fig.5.

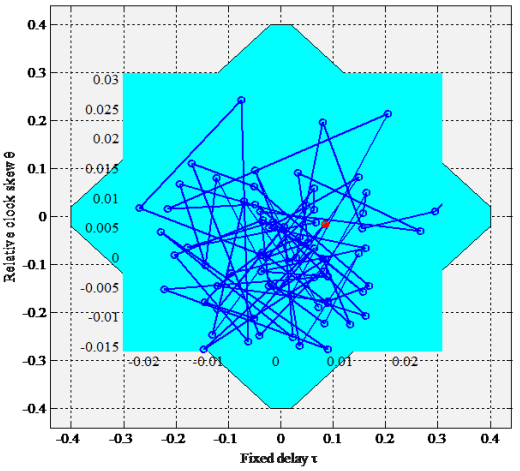

$$x(0) = [3; 2], Z = [0; 0]$$

FIGURE 5. State of disturbance system exponentially converged to set S.

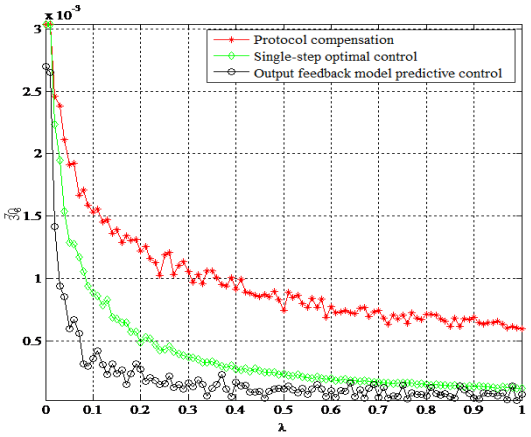

FIGURE 6. Comparison of convergent mean for synchronization error under different arrival rates.

C. ROBUST EXPONENTIAL CONVERGENCE UNDER DIFFERENT PACKET ARRIVAL RATES

(1) Fig.6 is shown for this section. We use the theory of incomplete measurement in section II to design a controller with certain robustness for packet loss in this paper, and quantify the control error. In order to reflect the effectiveness of control algorithm under different arrival rate of packets, we define the convergent mean of clock synchronization error as [3], [14]:

$$\bar{\theta}_\lambda = \frac{1}{M}\sum_{i=1}^{M}\bar{\theta}_i$$

where $\bar{\theta}_i = \frac{1}{N-l+1}\sum_{k=l}^{N}\theta_k$, N represents the number of exchange for clock message during a round of synchronization, and l indicates that θ_k reaches the range δ of convergence in step l and fluctuates within it. We assume that $\delta = \pm 4 * 10^{-4}$.

In order to simulate the situation of packet loss, the step size of arrival rate λ is set as 0.01. The sequence list of packet loss is generated randomly according to the arrival rate before experiments. Then code in binary system. This method simplifies the process of packet loss. The nodes carry out normal message exchange according to the complete measurement. When the corresponding sequence of packet loss is 0, then the packet will not be dealt with [2].

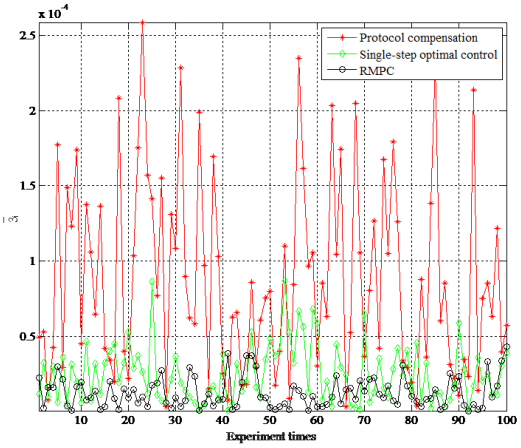

FIGURE 7. Comparison of convergent mean for synchronization error when $\lambda = 0.6$.

(2) Fig.7 is shown for this section. In each experiment about $\bar{\theta}_\lambda$, in order to show the stability of control in this paper, the data of $\bar{\theta}_{\lambda=0.6}$ in Fig.6 will be expanded to obtain the convergent mean $\bar{\theta}_i$ when arrival rate of packets is $\lambda = 0.6$, as shown in Fig.7. We can see that the fluctuation of $\bar{\theta}_i$ for protocol compensation is more severe and the fluctuation of $\bar{\theta}_i$ for single-step optimal control is second from Fig.7, while the fluctuation of $\bar{\theta}_i$ for the control algorithm of this paper is relatively small. Tubes-MPC can better adapt to the situation of packet loss.

(3) Fig.8 is shown for this section. In IV-D of this paper, we have proved that when there is packet loss and the arrival rate λ satisfies $\lambda_c < \lambda \leq 1$, the state of system with the output feedback model predictive control will converge exponentially to the positive invariant set centered at the target point Z.

In order to express the synchronization performance of the three algorithms in a random process $\bar{\theta}_i$ more clearly at the acceptance rate λ of packets, the synchronization process of two points λ=0.1 and λ=0.6 in Fig.6 is expanded. Fig.8 depicts the comparison of clock synchronization error $E(k)$ for protocol compensation, single-step optimal control, and output feedback model predictive control when arrival rate of packets are λ=0.1 and λ=0.6 respectively. When λ=0.1, the output feedback model predictive control declines rapidly in the first 7 steps and reaches -2×10^{-3} as shown in Fig.8 (a), then it reaches steady state in the following 36th step. However, at this point, the synchronization errors of single-step optimal control and protocol

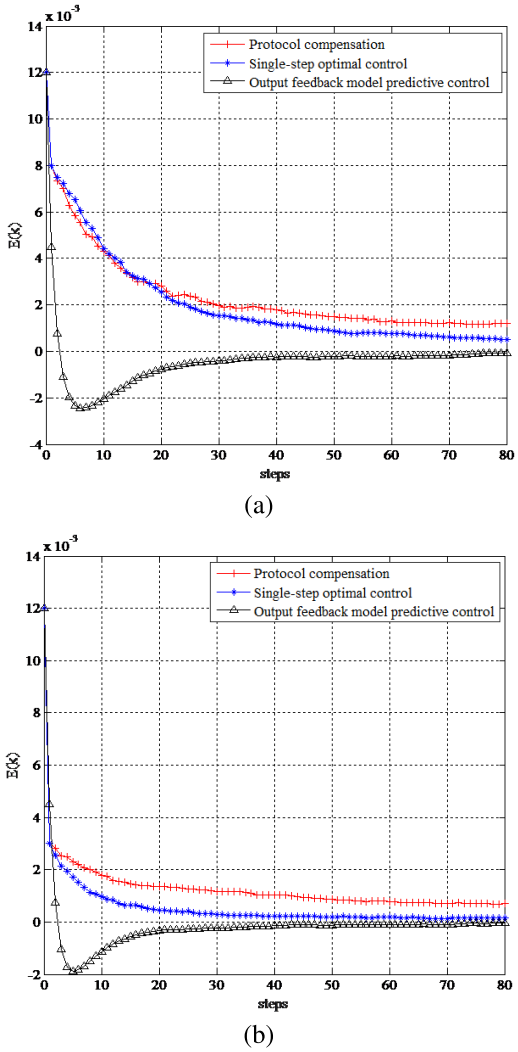

FIGURE 8. Comparison of synchronization error $E(k)$ with two different arrival rates.

compensation have not yet reached the steady-state. Finally, the synchronization errors of protocol compensation, single-step optimal control and output feedback model predictive control are respectively stable at 1.2×10^{-3}, 5.14×10^{-4} and -5.79×10^{-5}, which shows that the synchronization error of output feedback model predictive control is relatively low and it also has perfect synchronization performance at λ=0.1.

From Fig.8(b), the synchronization error of the output feedback model predictive control is still lower than the single-step optimal control, which is consistent with previous the conclusion in Fig.6.

In addition, it can be known from Fig.8(a) or Fig.8(b) that the synchronization error E(k) fluctuates within a very small range around 0 when the steady state is reachedč which is in accordance with the proof in IV-D that the state of system converges exponentially.

In summary, the algorithm proposed in this paper has better adaptability to packet loss.

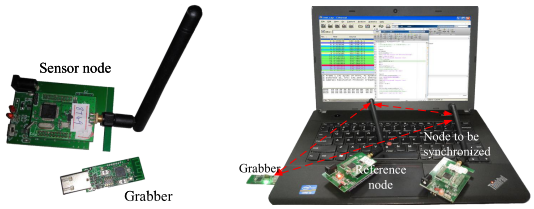

FIGURE 9. Sensor node, grabber and platform of experiments.

VI. EXPERIMENTAL TESTS AND ANALYSIS

The node configures STM32F103RB low-power microprocessors and Chipcon radio frequency chip CC2430/2431 (in Fig.9). It supports wireless standard of 2.4 GHz ISM band and IEEE802.15.4/ZigBee, the highest transfer rate of data is 250kbps. TimerA configures to use a 32MHz crystal oscillator divided by 4 as a clock source with as resolution. When the node reads the hardware clock, the CC2430/2431 will generate a time interrupt called Start Frame Delimiter (SFD) when the node sends or accepts the first byte of data packet.

The experimental platform consists of three nodes and one host computer. The nodes are grabber, reference node and node to be synchronized respectively. The grabber is equipped with a USB interface to connect directly to the host computer, all of the message and node status of the process during two-ways message exchange are grabbed by it. The grabber transmits the message and node status to the host computer and analyzes them by using Matlab. The data packets are mainly intercepted by using tools for visual grouping capture. We adjust the logic clock of nodes after synchronization algorithm is finished. This logic clock is maintained by the underlying service function of nodes.

In order to verify the long-term synchronization effect of algorithm on an actual network, it performs clock synchronization every 6 hours and implements the two-ways clock message exchange of clock synchronization 80 times at each turn in the synchronization environment of networked platform in Fig.8, and each interval of exchange time is 1s. The microprocessor can execute 2.77×10^5 instruction during this period (by a command is equal to three machine cycles to calculate), to ensure that it can finish the algorithm of clock synchronization. The grabber uploads packets every 5s. The distribution for convergent mean of synchronization error of network in 20 days is shown in Fig.10, and the statistical results are shown in Table 2. The smaller the standard deviation, the smaller the fluctuation of convergent mean for the synchronization error of the clock. We can define the normal error as:

$$D(\bar{\theta}_i) = \sqrt{1/M \sum_{i=1}^{M} [\bar{\theta}_i - E(\bar{\theta}_i)][\bar{\theta}_t - E(\bar{\theta}_i)]}$$

It can be seen quantitatively that the standard deviation of the convergence gain for the synchronization error of the clock of the Tube-MPC is smaller than the protocol compensation and single-step optimal control from Table 2,

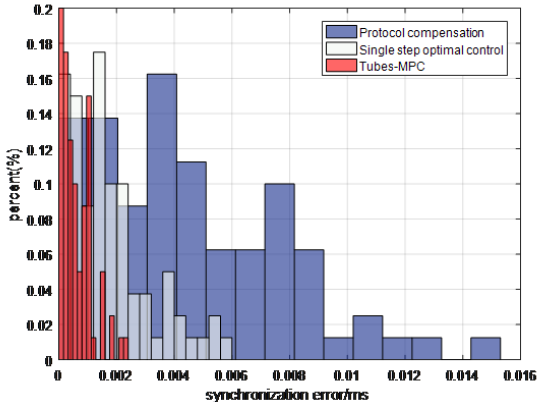

FIGURE 10. Distribution of 20 days convergent mean synchronization error under the experiment platform.

TABLE 2. Comparison of statistical results for the convergent mean of the synchronization error in the three algorithms.

Algorithm/μs	Mean	Standard deviation	Max	Min
Protocol compensation	4.61	3.31	15.26	0
Single step optimal control	1.78	1.45	5.95	0
Tubes-MPC	0.69	0.58	2.32	0

and the range of fluctuation is mainly concentrated in the area $[0, 0.002]$. The experiment has two practical aspects, on the one hand, it reflects the effect of the long-term clock synchronization, which has a lower clock fluctuation and a lower synchronization error and ensures the stability of the platform operation. On the other hand, the better synchronization maintainability in this paper can reduce the use of synchronous networked packet exchange and reduce networked traffic load.

VII. CONCLUSION

According to the observation model in incomplete measurement, the applicability of the control of the clock synchronization error for output feedback Tubes-MPC is verified by simulation experiments and the performance of exponentially stable convergence is obtained.

For the multi-node IIOT(Industrial Internet of Things) [18], the analyzing framework based on the output feedback model predictive control which is local and non-cooperative can be extended to the state-space model of the absolute clock by using a unified approach under the analysis of the packet loss in incomplete measurement. The controllable exponential convergence of clock synchronization for unreliable wireless network can be realized.

APPENDIX A
EXPONENTIAL CONVERGENCE UNDER UNRELIABLE BOUNDARY

The inference of Lemma 2: *The Set of State Estimated Error with Packet Loss*

There is a positive definite set $\tilde{S}^+$ for estimated error (39). If the initial state of disturbance system and estimated system satisfies $\tilde{x}(0) = x(0) - \hat{x}(0) \in \tilde{S}^+$.

Proof: Lemma 2 is based on the case of full measurement, but it can be seen from the above discussion, when considering packet loss, there are:

$$\tilde{x}_k(i) \in \tilde{S}^+ \supseteq \tilde{S}$$

As can be seen from Section III, the expectation of error covariance $E[P_k]$ satisfies:

$$0 < \bar{S} = \lim_{k\to\infty} S_k \le E[P_k] \le \lim_{k\to\infty} V_k = \bar{V}$$

where $\bar{S}$ and $\bar{V}$ can be calculated and they are the solution of equations $\bar{S} = (1-\lambda)A\bar{S}A^T + Q$ and $\bar{V} = g_\lambda(\bar{V})$ respectively. The boundary of $E[P_k]$ reflects a measurement of the deviation between the state of estimated system $\hat{x}$ and the state of disturbance system x. Define node S_i satisfies $x_i \in X$, and the set X contains the global logical virtual clock Z. When a packet loss occurs, according to the assumptions, there are:

$$\varphi(-\sqrt{V_k}) \le x_k(i) - \hat{x}_k(i) \le \varphi(\sqrt{V_k}), x_k(i) \in X, \forall i \in N_{N_c-1}$$

where $\varphi(\cdot)$ is the column vector composed of data corresponding to the upper left corner and the lower right corner of the input matrix obtained by function mapping. It can be known from the definition of positive invariant set that $\left[\varphi\left(-\sqrt{\bar{V}}\right), \varphi\left(\sqrt{\bar{V}}\right)\right]_{1-\lambda}$ is a positive definite set of $\tilde{x}_k(i) = x_k(i) - \hat{x}_k(i)$ with the corresponding rate of packet loss $1-\lambda$. For the functional relationship of different rate of packet loss and upper bound of covariance, the set $\tilde{S}$ is expanded to $\tilde{S}^+$ with the corresponding rate of packet loss $1-\lambda$, that is $\left[\varphi\left(-\sqrt{\bar{V}}\right), \varphi\left(\sqrt{\bar{V}}\right)\right]_{1-\lambda}$, and there are:

$$\tilde{S}^+ - \tilde{S} = \Delta$$

Then $\tilde{S}^+$ is the positive invariant set of the estimated error with packet loss. According to Lemma 2, the inference of Lemma 2 with packet loss can be obtained.

The inference of Lemma 3: *The Set of Control Error with Packet Loss*

In the case of considering packet loss, for the control error (42), if the initial state of estimated system and the nominal system satisfies $e(0) = \hat{x}(0) - \bar{x}(0) \in \bar{S}$č then there are still $e(k) \in \bar{S}$, i.e. $\hat{x}(k) \in \bar{x}(k) \oplus \bar{S}$ for $\forall w_k \in W$ and $\forall v_k \in V$.

Proof: In the case of considering packet loss, the state update equation and observation equation of clock synchronization are as follows:

$$\begin{cases} x(k) = Ax(k-1) + Bu(k-1) + w_k \\ y(k) = \gamma_k[Cx(k) + v_k] \end{cases}$$

The expression of the Luenberger observer is:

$$\begin{cases} \hat{x}(k) = A\hat{x}(k-1) + Bu(k-1) + L[y(k-1) - \hat{y}(k-1)] \\ \hat{y}(k) = \gamma_k C\hat{x}(k) \end{cases}$$

where $\hat{x}(k)$ is the observation state at the current k time, L is the observer gain. The differential equation of the control error $e(k)$ for estimated system and nominal system is:

$$\begin{aligned} e(k) &= \hat{x}(k) - \bar{x}(k) \\ &= A_{\bar{K}} e(k-1) + \gamma_{k-1}[LC\tilde{x}(k-1) + Lv_{k-1}] \end{aligned}$$

where $A_{\bar{K}} \triangleq A + B\bar{K}$, $\bar{\delta}(k-1) \triangleq \gamma_{k-1}[LC\tilde{x}(k-1) + Lv_{k-1}]$, $\rho(A_{\bar{K}}) < 1$. Iterating over the above equations, there are:

$$e(k) = A_{\bar{K}}^k e(0) + \sum_{j=0}^{k-1} A_{\bar{K}}^j \bar{\delta}_{k-1-j}$$

where $e(0) = \hat{x}(0) - \bar{x}(0)$. When $e(0) = 0$, $e(k) \in \bar{S} = \sum_{j=0}^{k-1} A_{\bar{K}}^j \overline{\Delta} = \overline{\Delta} \oplus A_{\bar{K}}\overline{\Delta} \oplus \cdots \oplus A_{\bar{K}}^j \overline{\Delta}$, $\overline{\Delta} = \gamma_{k-1}[LC\tilde{S} \oplus LV]$, then $e(k) \in \bar{S}$ can be proved. Therefore, whether or not the packet loss occurs, a robust positive invariant set $\bar{S}$ of control error can be calculated in a finite time, and $\bar{S}$ is a compact set.

The inference of Lemma 4: *The Set of Interference Error with Packet Loss*

In the case of considering packet loss, there are $S^+ \triangleq \tilde{S}^+ \oplus \bar{S}$. If the initial error is $\tilde{x}(0) \in \tilde{S}^+$ and $e(0) \in \bar{S}$, there are $x(k) \in \hat{x}(k) \oplus \tilde{S}^+ \subseteq \bar{x}(k) \oplus S^+$ with control $u(k) = \bar{u}(k) + \bar{K}e(k)$.

Proof: According to the inference of Lemma 2, the inference of Lemma 3 and the operation rule of Minkowski set, it is clearly that the inference of Lemma 4 is established.

Lemma 5: If conditions (37)(38) holds, and $\bar{x}(k) \in \bar{X}_{N_c}$, then for the objective function there are [16]:

$$V_{N_C}^0(\bar{x}(k+1)) \le V_{N_C}^0(\bar{x}(k)) - \ell(\bar{x}(k), \bar{u}(k))$$

Lemma 6: Assuming that condition (38) is true, and for different objective functions $V_j^0(\bar{x}(k))$, j is an arbitrary integer. Given the same initial state $\bar{x}(k)$, then as j increases, the objective function is [20]:

(1) $V_{j+1}^0(\bar{x}(k)) \le V_j^0(\bar{x}(k))$, $\forall \bar{x} \in \bar{X}_{N_c}$, $\forall j \in \{0, 1, \cdots, N_c - 1\}$;

(2) $V_{N_c}^0(\bar{x}(k)) \le V_f(\bar{x}(k))$, $\forall \bar{x} \in X_f$

Lemma 7: If the stage function $\ell(\cdot)$ and the terminal cost function $V_f(\cdot)$ respectively satisfy:

$$\begin{aligned} \ell(\bar{x}(k), \bar{u}(k)) &\ge c_1|\bar{x}(k) - Z|^2, \forall \bar{x}(k) \in \bar{X}_{N_c}, \forall \bar{u}(k) \in \bar{U} \\ V_f(\bar{x}(k)) &\le c_2|\bar{x}(k) - Z|^2, \forall \bar{x}(k) \in X_f \end{aligned}$$

where c_1 and c_2 are a set of constants which satisfy $c_2 > c_1 > 0$.Then for $V_{N_c}^0(\bar{x}(k))$, there are the following properties [16]:

(1) $V_{N_c}^0(\bar{x}(k)) \ge c_1|\bar{x}(k) - Z|^2$, $\forall \bar{x}(k) \in \bar{X}_{N_c}$

(2) $V_f(\bar{x}(k)) \le c_2|\bar{x}(k) - Z|^2$, $\forall \bar{x}(k) \in X_f$

(3) $V_{N_c}^0(f(\bar{x}(k), \bar{u}(k))) \le V_{N_c}^0(\bar{x}(k)) - c_1|\bar{x}(k) - Z|^2, \forall \bar{x}(k) \in \bar{X}_{N_c}$

Proof: (1) According to the definition of the optimal problem for nominal system and the condition $\ell(\bar{x}(k), \bar{u}(k)) \ge c_1|\bar{x}(k) - Z|^2$, $V_{N_c}^0(\bar{x}(k)) \ge c_1|\bar{x}(k) - Z|^2$, $\forall \bar{x}(k) \in \bar{X}_{N_c}$ can be obtained.

(2) According to (2) in Lemma 6, there are $V^0_{N_c}(\bar{x}(k)) \leq V_f(\bar{x}(k))$ when $V^0_{N_c}(\bar{x}(k)) \leq V_f(\bar{x}(k))$. Combining condition $V_f(\bar{x}(k)) \leq c_2|\bar{x}(k) - Z|^2$, $V^0_{N_c}(\bar{x}(k)) \leq c_2|\bar{x}(k) - Z|^2$ can be obtained.

(3) According to lemma 5, there are $V^0_{N_C}(\bar{x}(k+1)) \leq V^0_{N_C}(\bar{x}(k)) - \ell(\bar{x}(k), u(k))$, that is:

$$V^0_{N_C}(\bar{x}(k+1)) - V^0_{N_C}(\bar{x}(k)) \leq -\ell(\bar{x}(k), \bar{u}(k)) \leq -c_1|\bar{x}(k) - Z|^2$$

So far, we have proved $V^0_{N_C}(\bar{x}(k+1)) \leq V^0_{N_C}(\bar{x}(k)) - c_1|\bar{x}(k) - Z|^2$.

REFERENCES

[1] C. C. Gami and K. J. Sarvakar, "Wireless sensor network: A survey," *Int. J. Res. Inf. Technol.*, vol. 1, no. 5, pp. 11–18, 2013.

[2] M. Epstein, L. Shi, A. Tiwari, and R. M. Murray, "Probabilistic performance of state estimation across a lossy network," *Automatic*, vol. 44, no. 12, pp. 3046–3053, 2008.

[3] S. Bolognani, R. Carli, E. Lovisari, and S. Zampieri, "A randomized linear algorithm for clock synchronization in multi-agent systems," *IEEE Trans. Autom. Control*, vol. 61, no. 7, pp. 1711–1726, Jul. 2016.

[4] S. Ahmed, F. Xiao, and T. Chen, "Asynchronous consensus-based time synchronisation in wireless sensor networks using unreliable communication links," *IET Control Theory Appl.*, vol. 8, no. 12, pp. 1083–1090, Aug. 2014.

[5] W. Ting, G. Di, C. Chun-Yang, T. Xiao-Ming, and W. Heng, "Clock synchronization in wireless sensor networks: Analysis and design of error precision based on lossy networked control perspective," *Math. Problems Eng.*, vol. 2015, Mar. 2015, Art. no. 346521.

[6] B. Sinopoli, L. Schenato, M. Franceschetti, K. Poolla, M. I. Jordan, and S. S. Sastry, "Kalman filtering with intermittent observations," *IEEE Trans. Autom. Control*, vol. 49, no. 9, pp. 1453–1464, Sep. 2004.

[7] S. Ganeriwa, R. Kumar, and M. B. Srivastava, "Timing-sync protocol for sensor networks," in *Proc. Int. Conf. Embedded Networked Sensor Syst.* New York, NY, USA: ACM, 2004, pp. 138–149.

[8] J. Elson, L. Girod, and D. Estrin, "Fine-grained network time synchronization using reference broadcasts," *ACM SIGOPS Operating Syst. Rev.*, vol. 36, no. SI, pp. 147–163, 2002.

[9] M. Maróti, B. Kusy, G. Simon, and Á. Lédeczi, "The flooding time synchronization protocol," in *Proc. 2nd Int. Conf. Embedded Networked Sensor Syst.*, 2004, pp. 39–49.

[10] Y.-C. Wu, Q. Chaudhari, and E. Serpedin, "Clock synchronization of wireless sensor networks," *IEEE Signal Process. Mag.*, vol. 28, no. 1, pp. 124–138, Jan. 2011.

[11] L. Schenato and F. Fiorentin, "Average TimeSynch: A consensus-based protocol for clock synchronization in wireless sensor networks," *Automatica*, vol. 47, no. 9, pp. 1878–1886, Sep. 2011.

[12] A. Ahmad, D. Zennaro, E. Serpedin, and L. Vangelista, "A factor graph approach to clock offset estimation in wireless sensor networks," *IEEE Trans. Inf. Theory*, vol. 58, no. 7, pp. 4244–4260, Jul. 2012.

[13] A. Ahmad, D. Zennaro, E. Serpedin, and L. Vangelista, "Time-varying clock offset estimation in two-way timing message exchange in wireless sensor networks using factor graphs," in *Proc. IEEE Int. Conf. Acoust., Speech Signal Process.*, Mar. 2012, pp. 3113–3116.

[14] W. Ting, C. Chun-Yang, G. Di, T. Xiao-Ming, and W. Heng, "Clock synchronization in wireless sensor networks: A new model and analysis approach based on networked control perspective," *Math. Problems Eng.*, vol. 2014, Aug. 2014, Art. no. 731980.

[15] L. Schenato, B. Sinopoli, M. Franceschetti, K. Poolla, and S. S. Sastry, "Foundations of control and estimation over lossy networks," *Proc. IEEE*, vol. 95, no. 1, pp. 163–187, Jan. 2007.

[16] D. Q. Mayne, M. M. Seron, and S. V. Raković, "Robust model predictive control of constrained linear systems with bounded disturbances," *Automatica*, vol. 2, no. 2, pp. 219–224, 2005.

[17] D. Q. Mayne, S. V. Raković, R. Findeisen, and F. Allgöwer, "Robust output feedback model predictive control of constrained linear systems," *Automatica*, vol. 42, no. 7, pp. 1217–1222, Jul. 2006.

[18] T. Wang, X. Q. Xu, and X. M. Tang, "Scalable clock synchronization analysis a symmetric noncooperative output feedback tubes-MPC approach," *IEEE/CAA J. Automatica Sinica*, to be published.

[19] L. Shi, L. Xie, and R. M. Murray, "Kalman filtering over a packet-delaying network: A probabilistic approach," *Automatica*, vol. 45, no. 9, pp. 2134–2140, 2009.

[20] D. Q. Mayne and J. B. Rawlings, "Correction to 'Constrained model predictive control: Stability and optimality,'" *Automatica*, vol. 36, no. 3, p. 483, 2001.

[21] K. Ilya and E. G. Gilbert, "Theory and computation of disturbance invariant sets for discrete-time linear systems," *Math. Problems Eng.*, vol. 4, no. 4, pp. 317–367, 1998.

[22] B. Ding and Y. Yang, "A noncooperative distributed model predictive control for constrained linear systems with decoupled dynamics," in *Proc. 34th Chin. Control Conf.*, Hangzhou, China, Jul. 2015, pp. 4084–4090.

[23] P. Wang and B. Ding, "Distributed RHC for tracking and formation of nonholonomic multi-vehicle systems," *IEEE Trans. Autom. Control*, vol. 59, no. 6, pp. 1439–1453, Jun. 2014.

[24] B. Ding, L. Xie, and W. Cai, "Distributed model predictive control for constrained linear systems," *Int. J. Robust Nonlinear Control*, vol. 20, no. 11, pp. 1285–1298, 2010.

[25] X. Tang and B. Ding, "Model predictive control of linear systems over networks with data quantizations and packet losses," *Automatica*, vol. 49, no. 5, pp. 1333–1339, May 2013.

[26] X. Tang, H. Qu, P. Wang, and M. Zhao, "Constrained off-line synthesis approach of model predictive control for networked control systems with network-induced delays," *ISA Trans.*, vol. 55, no. 23, pp. 135–144, 2015.

[27] D. Mayne, "Robust and stochastic model predictive control: Are we going in the right direction?" *Annu. Rev. Control*, vol. 41, pp. 184–192, 2016.

TING WANG received the B.S. degree in mechanical engineering and the Ph.D. degree in mechatronic engineering from Southwest Jiaotong University, Chengdu, China, in 2001 and 2006, respectively. From 2007 to 2008, he was a Visiting Research Fellow with the National Power Traction Laboratory, Southwest Jiaotong University. Since 2006, he has been a Researcher with the Key Laboratory of Industrial Internet of Things and Networked Control, Ministry of Education, Chongqing University of Posts and Telecommunications (CQUPT), Chongqing. He is currently a Professor in control theory and control engineering with the Chongqing University of Posts and Telecommunications. His research interests include the industrial Internet of Things and wireless sensor networks, optimization, optimization based design, distributed model predictive control, networked control systems, and wireless data acquisition and data processing.

JIE SHANG received the B.S. degree from Hubei Polytechnic University, in 2017. She is currently pursuing the master's degree with the Automation College, Chongqing University of Posts and Telecommunications (CQOPT), majoring in the control engineering.

She is interested in model predictive control, clock synchronization, and so on.

XIAOMING TANG received the B.S. degree from the College of Information and Electrical Engineering, Panzhihua University, China, in 2008, and the Ph.D. degree from the College of Automation, Chongqing University, Chongqing, China, in 2013. From 2016 to 2017, he carried out his postdoctoral research with the University of Texas at Arlington, Arlington, TX, USA. He is currently an Associate Professor with the College of Automation, Chongqing University of Posts and Telecommunications, Chongqing. His research interests include model predictive control and networked control systems.